PROCEEDINGS OF SCIENCE

Antiproton Flux and Properties of Elementary Particle Fluxes in Primary Cosmic Rays Measured with the Alpha Magnetic Spectrometer on the ISS

Zhili Weng[*] **On behalf of AMS collaboration**

[a] *Massachusetts Institute of Technology (MIT), 77 Massachusetts Ave, Cambridge, MA 02139, United States*

E-mail: zhili.weng@cern.ch

We present the latest precision AMS measurements of the fluxes of all charged cosmic elementary particles, positrons, electrons, protons, and antiprotons based on the first 11 years of data collected on the International Space Station. These unique results, obtained with the same detector and with unprecedented precision in the uncharted energy range, provide precise experimental information and reveal new properties of cosmic charged elementary particles. In the absolute rigidity range of 60 to 525 GV, the antiproton-to-proton flux ratio is constant and the antiproton flux and proton flux have identical rigidity dependence. This behavior indicates an excess of high-energy antiprotons compared with secondary antiprotons produced from the collision of cosmic rays. More importantly, from 60 to 525 GV, the antiproton flux and positron flux also show identical rigidity dependence. The positron-to-antiproton flux ratio is independent of energy, and its value is determined to be a factor of 2 with percent accuracy. This unexpected observation indicates a common origin of high-energy antiprotons and positrons in the cosmos.

38th International Cosmic Ray Conference (ICRC2023)
26 July - 3 August, 2023
Nagoya, Japan

[*] Speaker

PoS(ICRC2023)1403

Introduction

Cosmic ray electrons, protons, positrons, and antiprotons are elementary particles in the cosmos that have infinite live time and travel through space indefinitely. In traditional cosmic-ray theory, protons and electrons are accelerated in supernova remnants together with other primary cosmic-ray nuclei. These particles interact with interstellar matter and produce a small amount of secondary positrons and antiprotons. New physics phenomena, such as annihilation of dark matter particles [1–3] and acceleration in astrophysical objects [4] may produce cosmic-ray particles and antiparticles in equal amounts.

The Alpha Magnetic Spectrometer (AMS) [5] is a precision general-purpose particle physics detector on the International Space Station (ISS). Precision data from AMS [6] have shown that, at high energies, positrons predominantly originate either from dark matter annihilation or from other astrophysical sources. Different models for the production and acceleration of high-energy positrons, either from dark matter [1–3] or from new astrophysical sources [4], present different predictions for cosmic-ray antiprotons on top of the traditional secondary antiprotons component. The precision measurement from AMS of the energy dependence of the antiproton flux and comparison with other elementary particle fluxes[6–10] provide new insight into the understanding of cosmic rays and new physics phenomena.

Antiprotons measured with AMS

The cosmic ray antiproton flux is about 1 in 10,000 of the proton flux. Precision measurement with a percent level accuracy requires a background rejection close to 1 in a million. The combination of information from different subdetectors of AMS enables the efficient separation of the antiproton signal from different background events. The full description of the AMS detector is presented in [5] and references therein. The tracker, together with the magnet, measures rigidity R (momentum/charge) and the charge sign of cosmic rays. For $|Z| = 1$ particles the maximum detectable rigidity, MDR, is 2 TV. It also measures the particle charge $|Z|$. The TOF counters measure $|Z|$ and velocity with a resolution of $\Delta\beta/\beta^2 = 4\%$. It is used to identify $\bar{p}(p)$ from light particles ($e^{\pm}$ and $\pi^{\pm}$) below 4 GV. The ring imaging Čerenkov detector, RICH, has a velocity resolution $\Delta\beta/\beta = 0.1\%$ for $|Z| = 1$ particles. It is used to identified $\bar{p}(p)$ from light particles ($e^{\pm}$ and $\pi^{\pm}$) below 10 GV. To distinguish antiprotons from proton reconstructed in the tracker with negative rigidity, a charge confusion estimator Λ_{CC} is defined by combining information from the tracker and TOF using the boosted decision trees technique [11]. The transition radiation detector, TRD, identifies $\bar{p}(p)$ from $e^-(e^+)$ background. The ECAL is a 3-dimensional imaging calorimeter with 17 radiation length, which accurately measures $e^{\pm}$ energy and the shape of the shower. When the particle enters the acceptance of the ECAL, the ECAL is used to reject the $e^-(e^+)$ background. The analysis technique and procedure for cosmic ray antiprotons follow those described in [7]. In the first 11 years of AMS operation, more than 1.1×10^6 antiproton particles have been identified in the absolute rigidity range of 1-525 GV. This enables a precision study of properties of the antiproton flux.

In this contribution, the latest AMS measurements of proton flux (Φ_p), electron flux (Φ_{e^-}), positron flux (Φ_{e^+}), and antiproton flux ($\Phi_{\bar{p}}$) as functions of energy (E) or rigidity (R) are presented.

Data points are placed at $\tilde{E}$ (or $\tilde{R}$) calculated for a flux $\propto E^{-3}$ (or R^{-3}) [12]. For display purposes, we present the particle spectrum, i.e., the fluxes scaled by $\tilde{E}^3$ (or $\tilde{R}^3$), resulting in $\tilde{E}^3\Phi$ (or $\tilde{R}^3\Phi$).

Cosmic Elementary Particle Fluxes

Electrons and protons are the most abundant elementary particles in the cosmos. The latest AMS electron spectrum and the proton spectrum as functions of energy are presented in Figure 1(a). As seen, these two particles have distinctly different energy dependencies, in particular, above 10 GeV, electrons exhibit significantly softer energy dependence compared to protons. This is commonly attributed to energy losses by electrons during propagation in interstellar media.

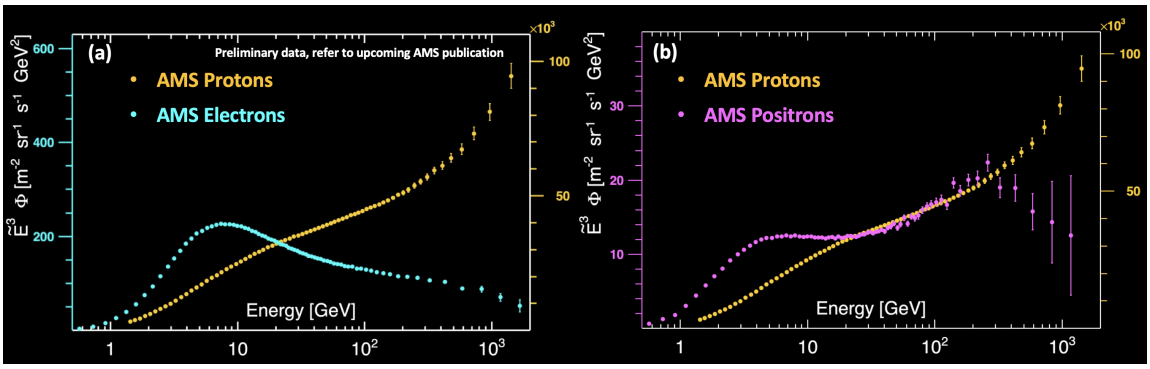

Figure 1: (a) The AMS electron spectrum, $\tilde{E}^3\Phi_{e^-}$, (blue data points, left axis) and proton spectrum, $\tilde{E}^3\Phi_p$, (orange data points, right axis) are shown as a function of energy. (b) The AMS positron spectrum, $\tilde{E}^3\Phi_{e^+}$, (magenta data points, left axis) and proton spectrum (orange data points, right axis) are shown as a function of energy.

The latest AMS measurements of the positron spectrum and proton spectrum are shown in Figure 1(b). A surprising observation is that the energy dependence of the positron spectrum is very similar to that of the proton spectrum in the energy range from 60 to ~260 GeV. This behavior is not expected from traditional cosmic-ray understanding in which positrons are of pure secondary origin. More importantly, the positron spectrum, $\tilde{E}^3\Phi_{e^+}$, decreases with increasing energy above ~260 GeV, in contrast to the proton spectrum, which progressively hardens around this energy [5, 8]. The complex energy dependence of the positron spectrum indicates that at high energies cosmic-ray positrons predominantly originate either from dark-matter collisions or from new astrophysical phenomena.

Antiproton flux and proton flux

The latest AMS measurements of the antiproton flux and the proton flux are shown in Fig.2. Unexpectedly, at absolute rigidity $|R|$ between 60 GV and 525 GV the functional behavior of the antiproton and proton are nearly identical. The $\bar{p}$/p flux ratio measured by AMS is shown in Fig.3. As seen, starting from 60 GV, the flux ratio is energy-independent up to 525 GV. This properties of cosmic antiproton are not expected from pure secondary antiprotons[14, 15] and indicates a primary source of antiproton, which may be of dark matter origin [1] or from other astrophysical sources [16].

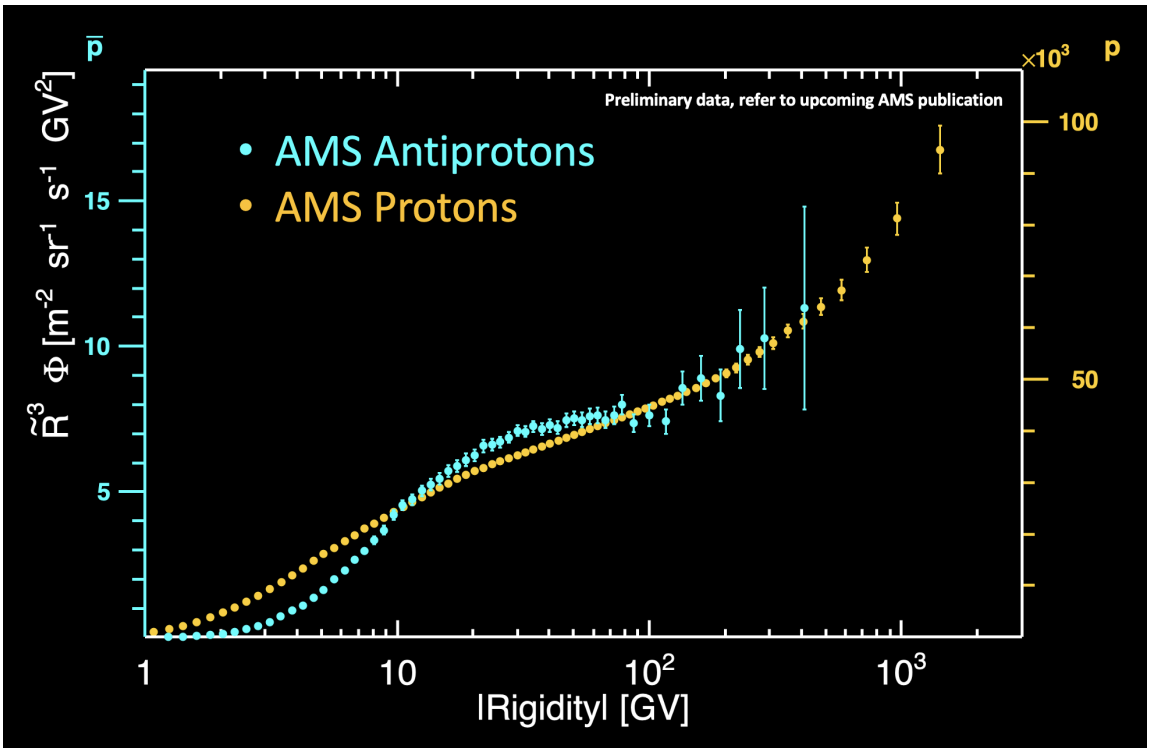

Figure 2: The AMS antiproton spectrum, $\tilde{R}^3\Phi_{\bar{p}}$, (blue data points, left axis) and AMS proton spectrum, $\tilde{R}^3\Phi_p$, (orange data points, right axis) are shown as a function of energy. Between 60 GV and 525 GV the functional behavior of the antiproton and proton are nearly identical.

After the first AMS publication on antiproton flux [7], there were many theoretical discussions to explain their unexpected behavior. The accuracy of the calculation of the flux of secondary cosmic-ray antiprotons was improved [17], and the theoretical discussion of the origin of high-energy antiprotons continues [18–21]. Among many examples, we present several recent models to illustrate the current understanding of the AMS results on antiprotons: Figure 4(a) shows the AMS antiproton spectrum and the antiproton-to-proton flux ratio together with two recent theoretical models that include only collisions of cosmic rays [22]. Figure 4(b) shows the AMS antiproton-to-proton flux ratio compared with a model predictions of antiprotons from dark matter and cosmic-ray collisions [23].

These recent studies reveal substantial model uncertainties that exceed the uncertainties of the AMS data. Future precision experimental data from AMS for different species and up to higher energy, as well as improved measurement of the $\bar{p}$ production cross section [17] are the key to reducing theoretical uncertainties in modeling antiprotons from collisions of cosmic rays. More importantly, future AMS measurements of the antiproton spectrum at the highest rigidity with improved accuracy, as well as its detailed time-dependent variations, will provide the most comprehensive data for understanding the origin of antiprotons in the cosmos.

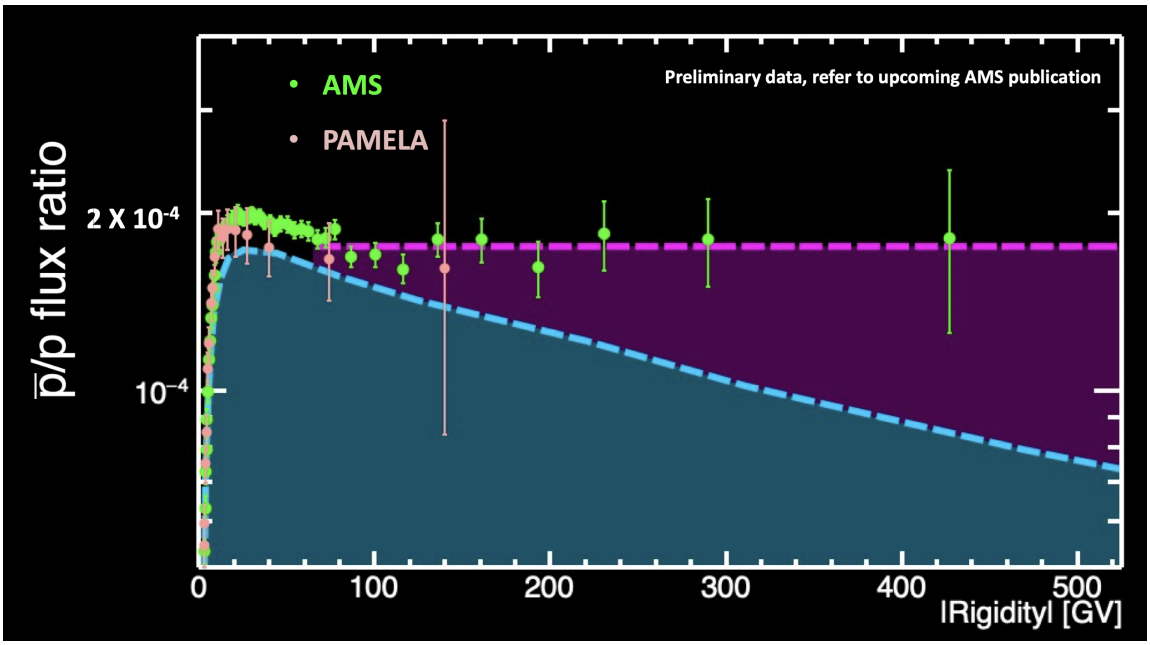

Figure 3: The latest AMS antiproton-to-proton flux ratio as a function of the absolute rigidity from 1 to 525 GV (green data point). The PAMELA [13] measurement is also shown (pink data point). The blue shaded area show the expected flux ration from antiproton produced in cosmic ray collisions[15].

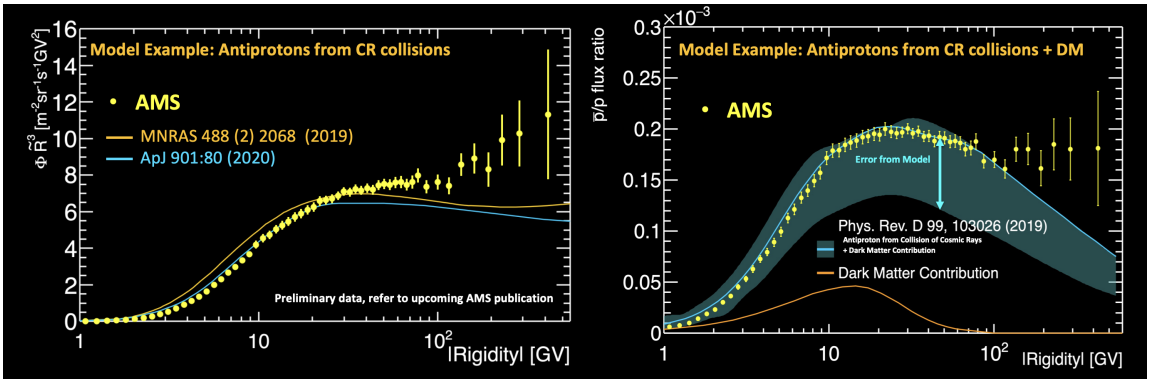

Figure 4: Example of recent theoretical models compared with the latest AMS data: (a) The AMS antiproton spectrum (yellow data points) together with two models that include only collisions of cosmic rays (solid lines). (b) The AMS antiproton-to-proton flux ratio (yellow data points) together with a model (blue lines), their uncertainties (blue bands), and the contributions from dark matter annihilation (orange lines)

Antiproton flux and positron flux

Cosmic positrons and antiprotons may have very different origin and propagation processes. Surprisingly, as shown in Fig.5, the AMS measurement of the positron flux and antiproton flux exhibit striking similarity in their energy dependence. The positron-to-antiproton flux ratio is shown in Fig.6. From 60 to 525 GeV, the flux ratio is compatible with being a constant. Fitting a constant to the flux ratio in this range yields $\Phi_{e^+}/\Phi_{\bar{p}} = 2.01 \pm 0.03(\text{stat.}) \pm 0.05(\text{syst.})$, consistent with a constant. Thus, the antiproton data show nearly identical energy dependence as positrons at high

energies.

The identical behavior of antiproton flux and positron flux are not expected from traditional cosmic ray models [14, 15] and indicates a common origin of high-energy antiprotons and positrons in the cosmos. Alternative models describing the production of secondaries from the interactions of cosmic ray nuclei with interstellar gas [24] are being confronted by the distinct energy dependence behavior of AMS measurements of cosmic elementary particles and nuclei. Antiprotons are not produced by pulsars; the existence of the cutoff in the antiproton energy spectrum is expected if high-energy antiprotons originate from dark-matter annihilation. The continuation of data taking through the lifetime of the ISS will provide important confirmation of the origin of high-energy positrons and antiprotons. A comprehensive model is required to explain the precision AMS measurement over a wide energy range, across different cosmic-ray species.

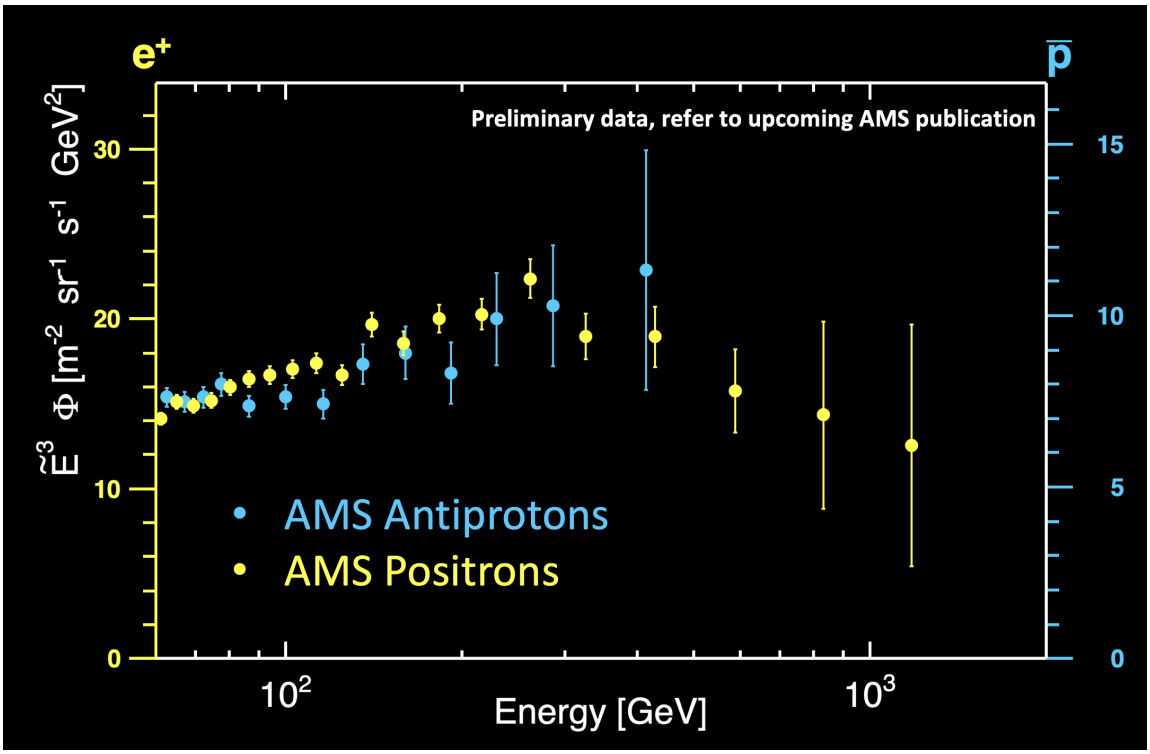

Figure 5: The AMS antiproton spectrum (blue data points, right axis) and the AMS positron spectrum (yellow data points, left axis) as a function of energy. Between 60 GeV and 525 GeV the functional behavior of the antiproton and proton are nearly identical.

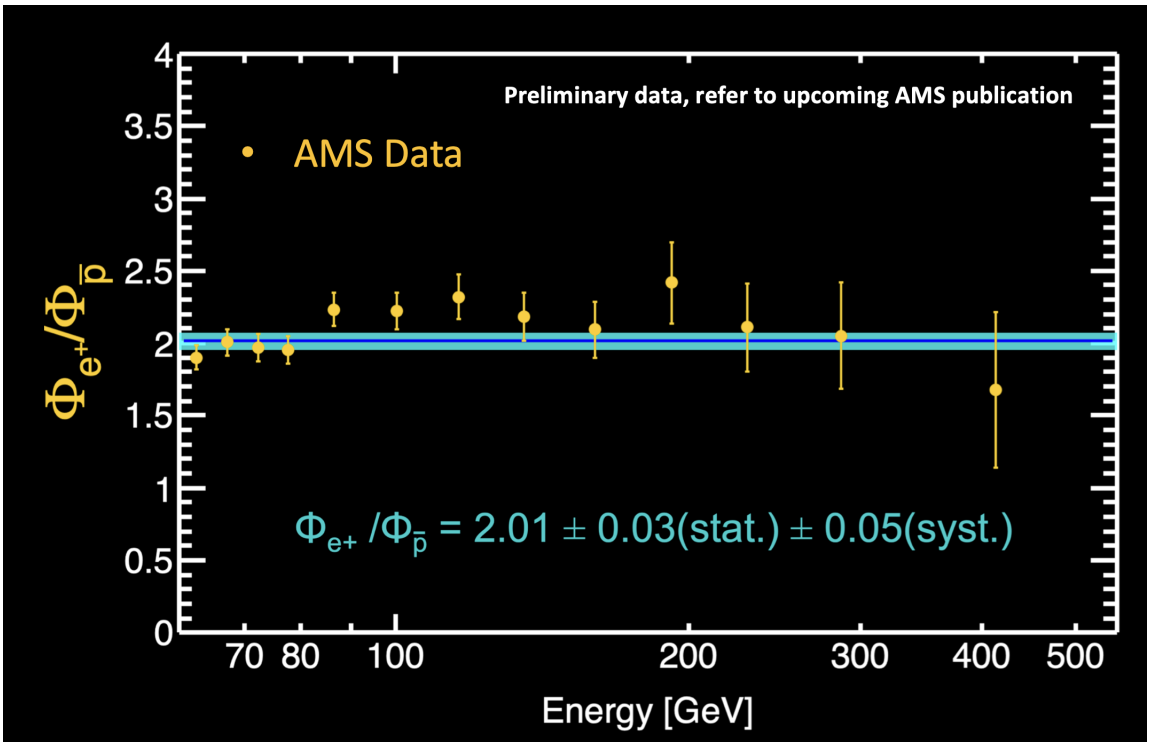

Figure 6: Positron-to-antiproton flux ratio measured by AMS (yellow data point). From 60 GeV to 525 GeV, the $e^+/\bar{p}$ flux ratio is compatible with a constant (blue line with 68% error band).

Conclusion

The latest precision AMS measurements of the fluxes of positrons, electrons, protons, and antiprotons reveal new properties of cosmic charged elementary particles. In the absolute rigidity range of 60 to 525 GV, the antiproton-to-proton flux ratio is constant and the antiproton flux and proton flux have identical rigidity dependence. This behavior indicates an excess of high-energy antiprotons in addition to secondary antiprotons produced from the collision of cosmic rays. More importantly, from 60 to 525 GeV, the antiproton flux and positron flux also show identical energy dependence. The positron-to-antiproton flux ratio is energy independent and the ratio is determined to be a factor of 2 with percent accuracy. This unexpected observation indicates a common origin of high-energy antiprotons and positrons in the cosmos. By collecting data through 2030, AMS will improve the accuracy of these measurements and extend to higher energy, providing unique data to understand the origin of antimatter particles in cosmic ray.

Acknowledgments

This work has been supported by individuals and institutions recognized in [5].

References

[1] F. Donato, *et al.*, Phys. Rev. Lett. **102**, 071301 (2009).

[2] J. Kopp, Phys. Rev. D **88**, 076013 (2013).

[3] Y. Bai, J. Berger, and S. Lu, Phys. Rev. D **97**, 115012 (2018).

[4] T. Linden and S.Profumo, Astrophys. J. **772**, 18 (2013).

[5] M. Aguilar, *et al.*, Physics Report **894**, 1 (2021).

[6] M. Aguilar, *et al.*, Phys. Rev. Lett. **110**, 141102 (2013); M. Aguilar, *et al.*, Phys. Rev. Lett. **113**, 121102 (2014); M. Aguilar, *et al.*, Phys. Rev. Lett. **122**, 041102 (2019); M. Aguilar, *et al.*, Phys. Rev. Lett. **122**, 101101 (2019).

[7] M. Aguilar, *et al.*, Phys. Rev. Lett. **117**, 091103 (2016) .

[8] M. Aguilar, *et al.*, Phys. Rev. Lett. **114**, 171103 (2015).

[9] M. Aguilar, *et al.*, Phys. Rev. Lett. **121**, 051101 (2018).

[10] M. Aguilar, *et al.*, Phys. Rev. Lett. **121**, 051102 (2018).

[11] B. Roe, *et al.*, Nucl. Instrum. Methods Phys. Res., Sect. A **543**, 577 (2005).

[12] G. Lafferty and T. Wyatt, Nucl. Instrum. MethodsPhys. Res., Sect. A 355, 541 (1995).

[13] O. Adriani,*et al.*, Phys. Rev. Lett. **102**, 051101 (2009); O. Adriani,*et al.*, Phys. Rev. Lett. **105**, 121101 (2010); O. Adriani,*et al.*, JETP Lett. **96**, 621 (2013).

[14] R. Trotta, *et al.*, Astrophys. J. **729**, 106 (2011).

[15] G. Jóhannesson, *et al.*, Astrophys. J. **824**, 16 (2016).

[16] P. Blasi and P.D. Serpico, Phys. Rev. Lett. **103**, 081103 (2009).

[17] M. Kachelriess, I. Moskalenko, and S. Ostapchenko, Astrophys. J. **803**, 54 (2015); M. Winkler, J. Cosmol. Astropart. Phys. 02 048, (2017).

[18] M. Kachelriess, A. Neronov, and D.V. Semikoz, Phys. Rev. Lett. **115**, 181103 (2015).

[19] P. Mertsch and S. Sarkar, Phys. Rev. D **90**, 061301 (2014); P. Mertsch, A. Vittino, S. Sarkar, Phys. Rev. D **104**, 103029, (2021).

[20] I. Cholis, D. Hooper, and T. Linden, Phys. Rev. D **95**, 123007 (2017).

[21] A. Cuoco, M. Krämer, and M. Korsmeier, Phys. Rev. Lett.,**118** 191102 (2017); M. Cui *et al.*, Phys. Rev. Lett.,**118** 191101 (2017).

[22] V. Bresci *et al.*, Mon. Not. R. Astron. Soc., 488, 2068 (2019); H. Jin *et al.*, Astrophys. J. **901**, 80 (2020).

[23] I. Cholis, T. Linden, and D. Hooper, Phys. Rev. D, **99**, 103026 (2019).

[24] R. Cowsik and T. Madziwa-Nussinov, Astrophys. J. **827**, 119 (2016); P. Lipari, Phys. Rev. D **95**, 063009 (2017); K. Blum, R. Sato, and M. Takimoto, Phys. Rev. D **98**, 063022 (2018).